

The dynamical properties of the aromatic hydrogen bond in $\text{NH}_4(\text{C}_6\text{H}_5)_4\text{B}$ from quasielastic neutron scattering

Niina Jalarvo^{a)}

Department SF1, Hahn-Meitner Institut, Glienickerstrasse 100, D14109 Berlin, Germany

Arnaud Desmedt

Laboratoire de Physico-Chimie Moléculaire, UMR 5803 CNRS-Université de Bordeaux I, 351 Cours de la Libération, F33405 Talence Cedex, France

Ruep E. Lechner and Ferenc Mezei

Department SF1, Hahn-Meitner Institut, Glienickerstrasse 100, D14109 Berlin, Germany

(Received 27 July 2006; accepted 4 October 2006; published online 14 November 2006)

$\text{NH}_4(\text{C}_6\text{H}_5)_4\text{B}$ represents a prototypical system for understanding aromatic H bonds. In $\text{NH}_4(\text{C}_6\text{H}_5)_4\text{B}$ an ammonium cation is trapped in an aromatic cage of four phenyl rings and each phenyl ring serves as a hydrogen bond acceptor for the ammonium ion as donor. Here the dynamical properties of the aromatic hydrogen bond in $\text{NH}_4(\text{C}_6\text{H}_5)_4\text{B}$ were studied by quasielastic incoherent neutron scattering in a broad temperature range ($20 \leq T \leq 350$ K). We show that in the temperature range from 67 to 350 K the ammonium ions perform rotational jumps around C_3 axes. The correlation time for this motion is the lifetime of the “transient” H bonds. It varies from 1.5 ps at $T=350$ K to 150 ps at $T=67$ K. The activation energy was found to be 3.14 kJ/mol, which means only 1.05 kJ/mol per single H bond for reorientations around the C_3 symmetry axis of the ammonium group. This result shows that the ammonium ions have to overcome an exceptionally low barrier to rotate and thereby break their H bonds. In addition, at temperatures above 200 K local diffusive reorientational motions of the phenyl rings, probably caused by interaction with ammonium-group reorientations, were found within the experimental observation time window. At room temperature a reorientation angle of $8.4^\circ \pm 2^\circ$ and a correlation time of 22 ± 8 ps were determined for the latter. The aromatic H bonds are extremely short lived due to the low potential barriers allowing for molecular motions with a reorientational character of the donors. The alternating rupture and formation of H bonds causes very strong damping of the librational motion of the acceptors, making the transient H bond appear rather flexible. © 2006 American Institute of Physics. [DOI: 10.1063/1.2374888]

I. INTRODUCTION

Hydrogen bonding is based on an attractive intermolecular interaction that exists between two partial electric charges of opposite polarity. The π -electron cloud of the aromatic ring can attract a molecule or ion, where the hydrogen atom has a positive partial charge, and thus an *aromatic hydrogen bonding*¹ arises. Aromatic H bonding presents an unusual situation where the acceptor includes six carbon atoms, instead of just one atom, as in the case of ordinary H bonding. As a consequence of this particular arrangement, the dynamical properties of the aromatic H bonding are complex and not yet well understood.

Aromatic H bonds are found in a number of substances. The occurrence and the function of the aromatic H bonds in many biological systems, like in protein-DNA interactions, make this phenomenon exciting. With respect to the aromatic hydrogen bonds, $\text{B}(\text{C}_6\text{H}_5)_4^-$ (tetraphenylborate) salts are a remarkable substance class, presenting a quintessential example of π acceptors. Bakshi *et al.*² have calculated that in

$\text{B}(\text{C}_6\text{H}_5)_4^-$, each phenyl ring carries a delocalized partial charge of $0.19e$, making them very capable aromatic acceptors. In consequence tetraphenylborate salts have been extensively used as model systems for studies. The simplest member of this category, ammonium tetraphenylborate [$\text{NH}_4\text{B}(\text{C}_6\text{H}_5)_4$, hereafter called ATPB], is a prototypical system to understand aromatic H bonds. Steiner and Mason³ have characterized the structure of ATPB by neutron diffraction at 20 and 293 K. At both temperatures the structures are virtually identical, but the displacement parameters are much larger at room temperature. In Fig. 1 the structure of ATPB is presented. The boron atom is located in the center of the $\text{B}(\text{C}_6\text{H}_5)_4^-$ anion with the four phenyl rings attached around it. Two neighboring anions form an aromatic cage, inside which the NH_4^+ cation is located. Each of the $\text{N}^+ - \text{H} \cdots \text{Ph}$ interactions can form an aromatic H bond. The ATPB crystals have tetragonal unit cells, with point group $I4_2m$.

To better understand the dynamical properties of the aromatic H bond in ATPB, quasielastic incoherent neutron scattering⁴ (QINS) experiments were performed in a large temperature range. It is worth to point out here that QINS is an especially appropriate method for the study of the dy-

^{a)}Author to whom correspondence should be addressed. Electronic mail: niina.jalarvo@googlemail.com



FIG. 1. The structure of ATPB determined by neutron diffraction (Ref. 3). The ammonium ion is located between two tetraphenylborate cations. Each of the $N^+-H\cdots Ph$ interactions can form an aromatic H bond (indicated by dashed lines in the center of the figure).

namical properties of the ATPB molecules, because the latter contain many hydrogen atoms, which have the largest existing incoherent neutron scattering cross section. The diffusive motions of reorientation of the ammonium ions and the phenyl rings in ATPB are expected to occur in a time window accessible to the quasielastic neutron scattering (QENS) technique and the use of a sample with deuterated ammonium ions (hereafter called ATPB-D) allows one to practically exclude the motions of ammonium groups, because the incoherent scattering cross section of D is 39.2 times smaller than that of H.

II. EXPERIMENTAL DETAILS

The ATPB sample was prepared following the instruction of Westerhaus *et al.*⁵ Equimolar amounts of $Na(C_6H_5)_4B$ and NH_4Cl , both commercially available, were dissolved in water at room temperature. The white salt of ATPB precipitated immediately and it was washed with acetone for recrystallization. The ATPB-D sample was prepared from commercially available products: ND_4Cl and $Na(C_6H_5)_4B$. Equimolar amounts of these powders were separately dissolved in D_2O at room temperature in a closed argon atmosphere. After mixing the solutions a white salt of ATPB-D precipitates immediately. For recrystallization, the ATPB-D salt was subsequently washed with deuterated acetone $(CD_3)_2CO$. The exact chemical formula of the prepared ATPB-D sample was found to be $N(D_{0.77}H_{0.23})_4(C_6H_5)_4B$. Details of the procedure to determine the fraction of deuterated ammonium ions are given in Ref. 6. This result implies that the selective deuteration was not complete, and thus a contribution from the NH_4 groups is still observable although drastically reduced.

The QENS experiments were performed using the time-of-flight spectrometer NEAT (Refs. 7–9) at the Berlin Neutron Scattering Centre (BENS) of the Hahn-Meitner-Institut (HMI) in Berlin. The masses of the samples were about 0.6 g for ATPB and about 0.41 g for ATPB-D, resulting in transmission probabilities of 0.85 and 0.9, respectively. The samples were placed into a flat aluminum container with a thickness of 0.4 mm and examined in reflection geometry. In such a case the angle between the sample plane and the incident neutron beam was kept equal to 45° , allowing the observation of the low and the high angle region. The range of scattering angles (2θ) at the NEAT spectrometer varies from 13° to 136° . The corresponding momentum transfer values were obtained using the following expression: $\hbar Q = 4\pi \sin(2\theta)/\lambda_0$, where λ_0 is the incident neutron wave-

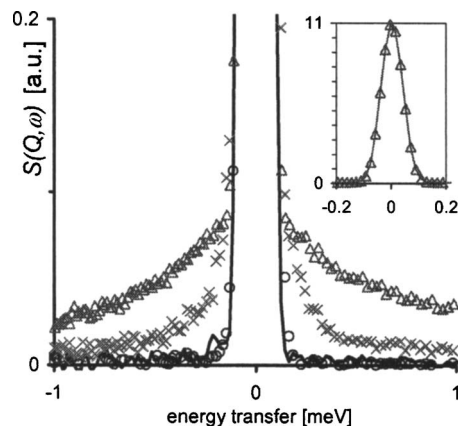


FIG. 2. Rescaled ATPB spectra are shown at three selected temperatures, 300 K (triangles), 100 K (crosses), and 20 K (circles), for the elastic Q value 2.1 \AA^{-1} and for $\Delta E = 98 \mu\text{eV}$. The solid line is the measured resolution function. The inset shows the corresponding elastic intensity at 300 K.

length. The QENS spectra for ATPB were recorded at several temperatures between 20 and 350 K. Two different incident neutron wavelengths, 5.1 and 8 \AA , were used, the former one having elastic instrument resolutions [full width at half maximum (FWHM)] of 56, 98, and 182 μeV and the latter one having 32 μeV . For ATPB-D the QENS spectra were recorded at 300 K using an incident neutron wavelength of 8 \AA . Data acquisition times varied between 24 and 6 h. In addition to elastic incoherent scattering, both samples yielded quasielastic incoherent scattering, suggesting the presence of localized diffusive motions which involve hydrogen atoms.

The NEAT raw data were corrected for detector efficiency and sample-geometry dependent attenuation. Additionally the background was subtracted using a measurement of the empty sample container. The data were normalized to the elastic scattering of vanadium and transformed to energy scale. Then several detectors were grouped together to improve the statistical accuracy. These procedures were carried out by the FITMO4 software.¹⁰

After the corrections and the conversion to energy scale, the experimental data are given as a function of momentum transfer ($\hbar Q$) and energy transfer ($\hbar\omega$) between the neutrons and the scattering system. An overview of the QENS spectra at three temperatures, 300, 100, and 20 K, is shown in Fig. 2. The observed relatively large elastic intensity, compared to the corresponding QE component, suggests that a large fraction of the hydrogen atoms in ATPB are immobile on the time scales observed in the NEAT experiments. Therefore, the first step in our data analysis was to consider that the phenyl rings are immobile and that the observed quasielastic component originates only from reorientations of the ammonium ions.

III. DATA ANALYSIS AND RESULTS

The extracted experimental spectra originate mainly from the incoherent scattering of the hydrogen atoms in the ATPB powder. Coherent contributions to the scattered intensity are negligible, since Bragg peaks were carefully removed from the experimental data and coherent inelastic

scattering is well separated from the quasielastic region of the spectra. The inelastic contributions are taken into account as a background term, in the quasielastic region in which we are interested in the frame of this work. The connection between the measured neutron scattering spectra and the incoherent scattering function and, in particular, for diffusive atomic motions is described, e.g., in Refs. 11 and 12. It is not expected that translational diffusion in ATPB would occur on the time scale accessible by the NEAT measurements. Instead, it may be expected that local diffusive reorientational motions of ammonium and phenyl groups are the source of the observed quasielastic scattering. The incoherent scattering function for such a case can be written as follows:

$$S_{\text{inc}}(Q, \omega) = e^{-\hbar\omega/2kT} [e^{-(u^2)Q^2} R(Q, \omega) + B(Q, \omega)], \quad (1)$$

where $e^{-\hbar\omega/2kT}$ is the detailed balance factor, $e^{-(u^2)Q^2}$ is the Debye-Waller factor, $R(Q, \omega)$ is the reorientational scattering function, and $B(Q, \omega)$ is the background term, which in the present case can be represented by a straight line, since the energy window considered is fairly small. The reorientational scattering function is concentrated on the elastic and quasielastic parts of the spectra, and it can be written as

$$R(Q, \omega) = A_0(Q) \delta(\omega) + \sum_{j=1}^n A_j(Q) L_j(\omega), \quad (2)$$

where $A_0(Q)$ is the elastic incoherent structure factor (EISF), $\delta(\omega)$ represents the elastic term with zero energy width (Dirac function), and $L_j(\omega)$ are the quasielastic contributions, each with its own quasielastic incoherent structure factor (QISF), $A_j(Q)$. The Lorentzians $L_j(\omega)$ read

$$L_j(\omega) = \frac{I}{\pi} \frac{\Delta_j}{\Delta_j^2 + \omega^2}, \quad (3)$$

where Δ_j is the half-width at half maximum (HWHM) connected to the time scale on which the motion occurs. In the analysis, when theoretical expressions are compared to the measured spectra, the whole function $R(Q, \omega)$ has to be folded with the experimental energy resolution function. This convolution is not shown explicitly here. If the resolution-broadened (sufficiently narrow) elastic component and the (sufficiently broad) quasielastic component can be experimentally separated, the EISF is a measurable quantity, evaluated from the ratio

$$\text{EISF}(Q) = \frac{I^{\text{el}}(Q)}{I^{\text{el}}(Q) + I^{\text{QE}}(Q)}, \quad (4)$$

where $I^{\text{el}}(Q)$ and $I^{\text{QE}}(Q)$ are the integrated elastic and quasielastic intensities. The EISF reveals information about the geometry of the reorientation.

A. Ammonium reorientations

The first step of the data analysis concerns phenomenological fits in order to find an appropriate model for the NH₄⁺ reorientations. In this case the structure factors EISF and QISF were fit parameters, as well as the width of the quasielastic component (Δ). The weight factors for both, elastic and quasielastic components, were defined assuming that the

phenyl rings would only contribute to the elastic part of the spectra. The reorientational scattering function for this phenomenological approach is therefore given by

$$R^{\text{NH}_4^+}(Q, \omega) = \left[\frac{5}{6} + \frac{1}{6} A_0(Q) \right] \delta(\omega) + \frac{1}{6} [1 - A_0(Q)] L_I(\omega), \quad (5)$$

where $A_0(Q)$ is the EISF and $(1 - A_0(Q))$ is the QISF. Subsequently, an approximate description of the reorientational motions of the NH₄⁺ ion can be derived from the fits by comparing the obtained experimental EISF values to theoretical ones.

Due to the tetrahedral symmetry of the NH₄⁺ ion, several specific models can be considered. The ammonium ion has three twofold axes (passing through the nitrogen) and four threefold axes (passing through the nitrogen atom and one of the hydrogen atoms). In the two-site jump model NH₄⁺ rotates around one of the C₂ axes and in the three-site jump model around one of the C₃ axes. Both of these models are described in the literature.^{11–15} In this special case, the obtained theoretical EISFs for both cases are identical because of two reasons: (i) one H atom is immobile in the case of the three-site jump model and (ii) the jump distance for both models is the same, the nearest-neighbor distance of protons in the ammonium group, $d_{\text{H-H}} = 1.708 \text{ \AA}$ (from crystallographic studies¹⁶):

$$A_0^{\text{NH}_4^+}(Q) = \frac{1}{2} [1 + j_0(Qd_{\text{H-H}})], \quad (6)$$

where j_0 is the spherical Bessel function of zeroth order. It is theoretically impossible to distinguish these two types of rotations of NH₄⁺ in ATPB, as the reorientational scattering functions for these cases are identical. The only difference is in the definition of the HWHM (Δ_j) of the quasielastic broadening, which is proportional to the jump rate τ^{-1} of the motion. For the two-site jump model this relation is given by

$$\Delta_2 = 2\tau_2^{-1}, \quad (7)$$

and for the three-site jump model it is given by

$$\Delta_3 = \frac{3}{2}\tau_3^{-1}. \quad (8)$$

A final remark may be done according to the $\bar{4}2m$ symmetry of the crystallographic site occupied by the ammonium ion.³ Such a symmetry would be respected by considering reorientations of the C₃ molecular axis. It follows that the EISF associated to such a model can be approximated by a tetrahedral jump model (T_d) given by^{17,18}

$$A_{04}(Q) = \frac{1}{4} \left[1 + 3j_0 \left(Q \frac{2\sqrt{2}}{\sqrt{3}} d_{\text{N-H}} \right) \right], \quad (9)$$

where $d_{\text{N-H}}$ is 1.046 Å (Ref. 16) and the HWHM Δ_4 and the jump rate τ_4^{-1} are related as follows:

$$\Delta_4 = \frac{4}{3}\tau_4^{-1}. \quad (10)$$

In Fig. 3, the EISF obtained from the fits of the phenomenological approach is shown in comparison with the above-mentioned theoretical models. It can be clearly seen that the T_d model does not reproduce the experimental data. This observation suggests that the reorientation of the C₃ molecular axis occurs on a time scale significantly slower than the

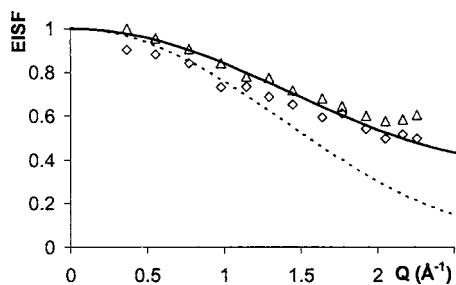


FIG. 3. Behavior of the EISF resulting from the fit at $T=200$ K with $\Delta E=98 \mu\text{eV}$ (circles) and $\Delta E=182 \mu\text{eV}$ (triangles) compared with a theoretical EISF. The solid line corresponds to rotation around the C_2 and C_3 axes. The dashed line corresponds to the T_d model (see text).

one probed in the present experiments. Instead, the experimental EISF was found to follow approximately the behavior of the two-site or three-site jump model. In ATPB, if the NH_4^+ is to rotate around a C_2 axis, all the four aromatic hydrogen

bonds have to be broken, while in the case of the rotation around a C_3 axis only three of these bonds would break. We therefore assume that the rotation around C_3 axes is preferable, because the energy needed for this process is likely to be only about 75% of that needed for the rotation around C_2 axes. Let us note here that this interpretation of the data is different from that given in Ref. 14, where the C_2 reorientational-jump process has been chosen.

Following the obtained premise, a second step in our data analysis was to fit the three-site jump model to the experimental spectra. The reorientational scattering function for the three-site jumps of the ammonium ion is obtained using Eq. (5), by replacing the EISF by the one for three-site jumps of NH_4^+ , as given in Eq. (6). The EISF is no longer a fit parameter and the HWHM is easily determined from the fit.

In Fig. 4, fit results of the three-site jump model are shown for three temperature regions high ($T > 200$ K), inter-

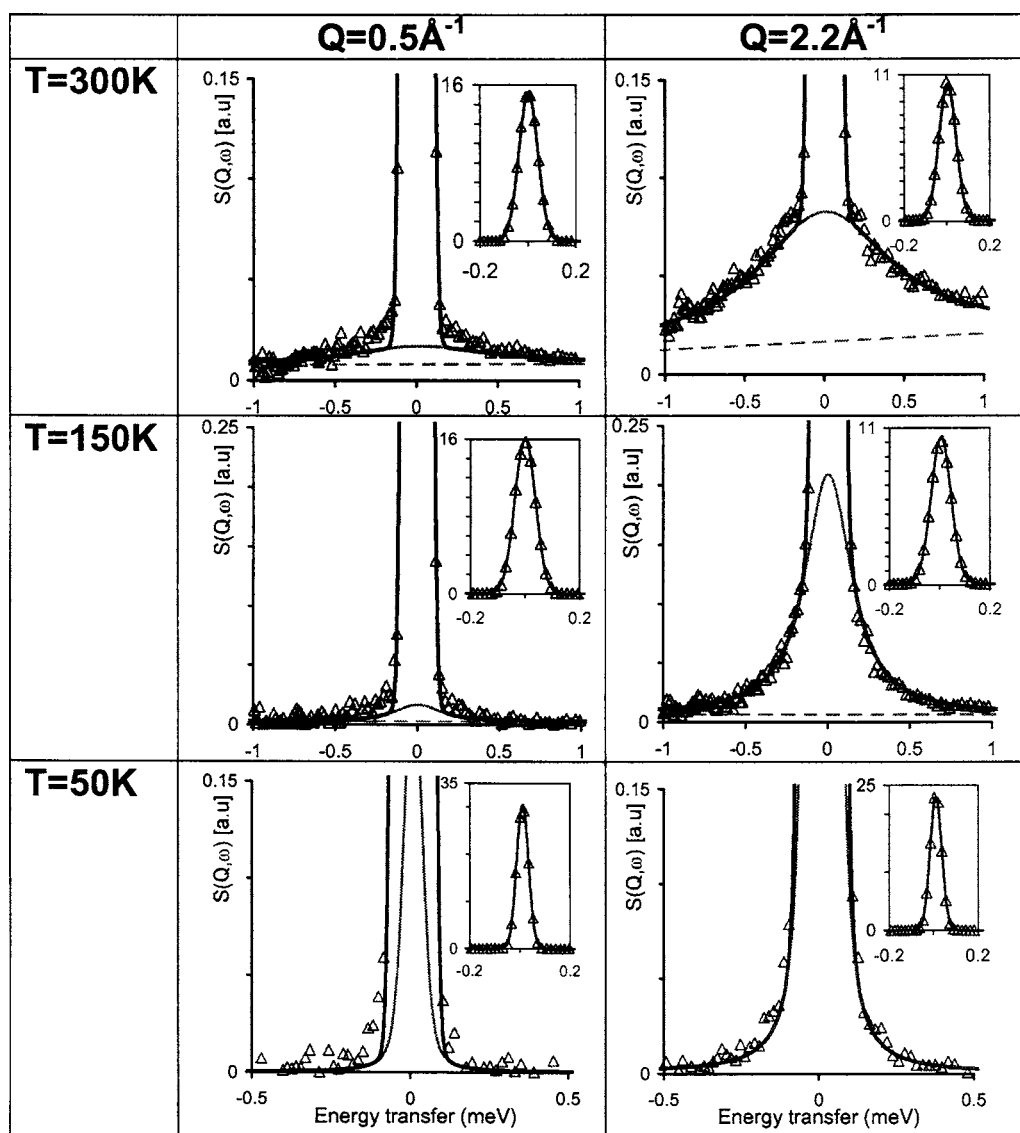


FIG. 4. The fitted three-site jump model is shown at two selected Q values 0.5 \AA^{-1} (left-hand side) and 2.2 \AA^{-1} (right-hand side), and at three selected temperatures, 300 K (on the top) and 150 K (middle) at $\Delta E=98 \mu\text{eV}$ and 50 K (on the bottom) at $\Delta E=56 \mu\text{eV}$. The triangles show the measured ATPB spectra. The dotted straight line is the fitted background and the Lorentzian shaped line is the fitted QE component. The entire fitted scattering functions are shown in the insets.

mediate ($200 \text{ K} > T > 67 \text{ K}$), and low ($T < 67 \text{ K}$), and at two selected Q values. In the low Q region deviations between the fit of this model and the experimental spectra were observed at each temperature. This is due to the multiple scattering (MSC) effect which can, in principle, be taken into account in the fit model. Anyhow, this rather complex procedure is not necessary for the interpretation of our data. Therefore, we merely refer to a previous work on the reorientational motion of ammonium groups in crystalline material under similar conditions, where the errors due to MSC have been evaluated.¹⁷ According to this, MSC-corrected spectra had larger correlation times by 3%–4%, but smaller activation energies by only 2%. Such error percentages will be applied below to correct our fit results. Our conclusion will be mainly based on data from the medium- to large- Q range, where the MSC effects are small as compared to the intensity of the quasielastic components. At medium- to large- Q range, the fit results are interpreted differently for the three temperature regions as follows.

1. $T > 200 \text{ K}$

In this temperature range the three-site jump model could not reproduce the total experimental QE intensity. Instead, differences are clearly seen near the elastic peak between the experimental data and the fitted model. The example for $T=300 \text{ K}$ at $\Delta E=98 \mu\text{eV}$ is shown in Fig. 4 (on the top). This observation indicates that one Lorentzian function, here that of the three-site jump model, is not sufficient to explain the obtained QE component. Indeed, an additional narrow QE component is needed to reproduce the experimental data accurately. As the width of the quasielastic component is inversely proportional to the correlation time of the proton dynamics in the sample, it can be assumed that the narrow component originates from a rather slow motion (compared to the ammonium ion reorientations). Reorientations of the phenyl rings are expected to be slower than the rotations of the ammonium ions, as a consequence of the 30 times larger momentum of inertia. Therefore the narrow component might originate from local diffusive reorientational motions of the phenyl rings. The possibility to explain this narrow component as a reorientation of the C_3 axes was already discussed in the context of the EISF fits and it was assumed not to be seen in the measured time scales. To investigate the origin of the additional quasielastic component, deuteration of the ammonium ions in ATPB was used as a tool.

2. $200 \text{ K} > T > 67 \text{ K}$

In this temperature region, the three-site jump model reproduces the experimental data well in the medium- to large- Q region, as, e.g., shown in Fig. 4 (middle) for $T=150 \text{ K}$ with $\Delta E=98 \mu\text{eV}$. The uncorrected jump rates vary from 0.2 meV at $T=200 \text{ K}$ to 0.0044 meV at 67 K (after MSC correction the jump rates vary from 0.19 to 0.0042 meV, respectively). The temperature dependence of the jump rate in this temperature region is shown in Fig. 5. The Arrhenius law, given by

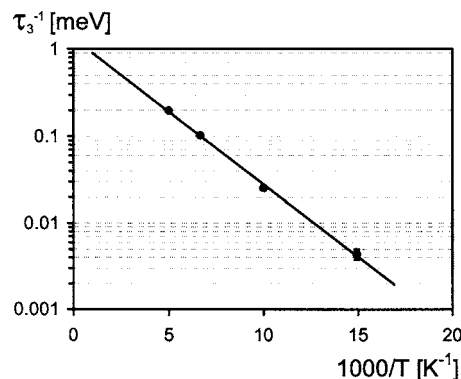


FIG. 5. Thermal evolution of the jump rate of the three-site jump model. The experimental points are represented by dots (not corrected for multiple scattering; see text concerning the corrections). The solid line is the fitted Arrhenius law.

$$\tau_3^{-1} = \tau_0^{-1} \exp(-E_a/k_B T), \quad (11)$$

where τ_3^{-1} is the jump rate, τ_0^{-1} the attempt frequency, E_a the activation energy, k_B Boltzmann's constant, and T the temperature, was fitted to the data points and the resulting uncorrected value of the activation energy is $3.2 \pm 0.1 \text{ kJ/mol}$. Application of the above-mentioned MSC correction then yields 3.14 kJ/mol .

3. $T < 67 \text{ K}$

At low temperatures the width of the quasielastic component is reduced, due to a slowing down of the diffusive motions. As a consequence another experimental observation time scale is needed. Therefore, for the low temperatures spectra were measured using a higher energy resolution, $\Delta E=56 \mu\text{eV}$. In Fig. 4 (bottom) an example at $T=50 \text{ K}$ is shown. It has to be noted that the experimental QE contribution is slightly broader than the one produced here by the fits. The deviations occur at the lower part on the sides of the elastic peak, which can be understood qualitatively by referring to a previous study of Roberts *et al.*,¹⁸ where tunneling of the ammonium ions in ATPB was observed at ± 26.5 and $\pm 53 \mu\text{eV}$. Our experimental energy resolution was not sufficient to properly separate these tunneling frequencies from the resolution function, but it is predictable that the tunneling frequencies cause a slight apparent "broadening" of the elastic line. The temperature dependence of tunneling and librational excited states of NH_4^+ in ATPB will be discussed more in detail in a forthcoming paper.¹⁹

B. Phenyl reorientations

In previous QENS studies of other solid compounds^{20–22} local diffusive reorientational motions of phenyl rings have been observed on a time scale of 10^{-11} – 10^{-9} s at room temperature. Therefore we used the elastic energy resolution of $32 \mu\text{eV}$ that corresponds to a time scale of about 10^{-10} s to measure the QENS spectra of ATPB and ATPB-D, in order to study the phenyl ring reorientations. Below, theoretical models for the local diffusive reorientations of the phenyl rings are presented. Subsequently, reorientational scattering func-

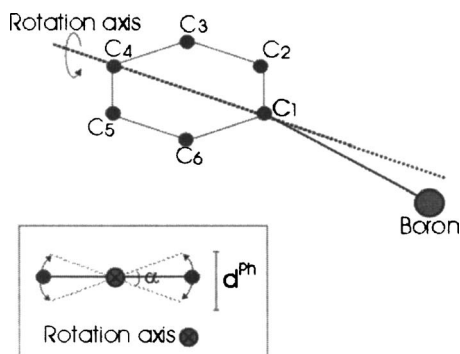


FIG. 6. The motions of the phenyl rings in ATPB can be described as a reorientation with respect to an axis, denoted as a dashed line in the larger figure. In the inset the phenyl ring is projected along the rotation axis; here the solid line represents the mean orientation of the phenyl ring and the dashed lines show the limits of the reorientation. The mobile atoms of the phenyl ring are jumping between those limits, in the model described here. The distance between the two limits of the motion is called the “jump distance,” denoted d^{Ph} in the sketch; α is the reorientation angle.

tions combining the phenyl ring and the ammonium ion reorientations are given and their fit to the experimental data is discussed.

The diffusive reorientations of the phenyl rings may originate from *a priori* librational motions of the rings, which at room temperature are, however, strongly damped due to the interaction with stochastically reorienting ammonium groups. They are described here, for simplicity, by a model of reorientational jump-diffusion with respect to the C_2 axis of the phenyl ring. According to this model the C_2 axis passes through two opposite corners of the phenyl ring, as shown in Fig. 6. The mobile atoms of the phenyl ring are assumed to hop between two positions, which are separated from each other by a distance d^{Ph} , as shown in the inset of Fig. 6. The EISF for this model is given by

$$A_{02}^{\text{Ph}}(Q) = \frac{1}{2}[1 + j_0(Qd^{\text{Ph}})]. \quad (12)$$

The analysis aims at finding a value for the reorientation angle α , which is connected to the distance d^{Ph} . Subsequently in our analysis, the reorientational motions of the phenyl rings as presented above are considered together with the ammonium ion reorientations around a C_3 axis. In this process three aromatic H bonds of each NH_4^+ unit are broken, while one remains intact. We assume here that breaking the aromatic H bonds leads to strongly damped librational motions of those phenyl rings which are involved in these bonds. Consequently, upon each reorientational jump of an ammonium group, one of the phenyl rings will not be incited to this motion, namely, that which at this instant is bound to the ammonium proton located on the rotation axis.

For the ATPB-D sample the rotational scattering function for such a model is given by

$$R^{\text{N(D}_{0.77}\text{H}_{0.23}\text{)}_4^+ \& \text{Ph}}(Q, \omega) = \left(\frac{5.3}{100} A_{03}^{\text{NH}_4^+} + \frac{52}{100} A_{02}^{\text{Ph}} + \frac{42.7}{100} \right) \delta(\omega) + \frac{5.3}{100} (1 - A_{03}^{\text{NH}_4^+}) \frac{1}{\pi} \frac{\Delta_{03}^{\text{NH}_4^+}}{\omega^2 + (\Delta_{03}^{\text{NH}_4^+})^2} + \frac{52}{100} (1 - A_{02}^{\text{Ph}}) \frac{1}{\pi} \frac{\Delta_{02}^{\text{Ph}}}{\omega^2 + (\Delta_{02}^{\text{Ph}})^2}, \quad (13)$$

where $A_{03}^{\text{NH}_4^+}$ and A_{02}^{Ph} are the EISFs and $\Delta_{03}^{\text{NH}_4^+}$ and Δ_{02}^{Ph} are the HWHMs for the rotation of the ammonium ions and the phenyl rings, respectively. The weight factors for the components are defined in the following way. The measured QE neutron scattering of the ATPB-D sample is dominated by the incoherent contribution of the hydrogen atoms. Although the deuteration of ammonium groups was not complete (77%), a drastic reduction of the incoherent contribution of the ammonium ions is expected. In order to obtain the right intensity factor for the deuterated ammonium ions, the coherent contribution has to be taken into account as well. The detailed theory describing the intensity distribution of coherent scattering is rather complex, but not really necessary for this analysis. Instead, a good approximation for the weight factor has been obtained by using the fraction of total scattering cross sections, $\sigma_{\text{tot}}(\text{ND}_{0.77}\text{H}_{0.23})/\sigma_{\text{tot}}(\text{ATPB-D}) = 0.053$. The intensity factor for the reorientations of the phenyl rings has been obtained by using the total scattering cross section percentage of the mobile protons (three phenyl rings and four hydrogens per ring) in the phenyl rings, $12\sigma_{\text{tot}}(\text{H})/\sigma_{\text{tot}}(\text{ATPB-D}) = 0.52$. The total scattering cross section of the mobile carbon atoms in the phenyl rings is negligible and therefore not considered here.

Analogously, the rotational scattering function for the ATPB sample, combining phenyl ring reorientations and ammonium ion rotations, is given by

$$R^{\text{NH}_4^+ \& \text{Ph}}(Q, \omega) = \left(\frac{4}{24} A_{03}^{\text{NH}_4^+} + \frac{12}{24} A_{02}^{\text{Ph}} + \frac{8}{24} \right) \delta(\omega) + \frac{4}{24} (1 - A_{03}^{\text{NH}_4^+}) \frac{1}{\pi} \frac{\Delta_{03}^{\text{NH}_4^+}}{\omega^2 + (\Delta_{03}^{\text{NH}_4^+})^2} + \frac{12}{24} (1 - A_{02}^{\text{Ph}}) \frac{1}{\pi} \frac{\Delta_{02}^{\text{Ph}}}{\omega^2 + (\Delta_{02}^{\text{Ph}})^2}, \quad (14)$$

where $A_{03}^{\text{NH}_4^+}$ and A_{02}^{Ph} are the EISFs and $\Delta_{03}^{\text{NH}_4^+}$ and Δ_{02}^{Ph} are the HWHMs for the rotation of the ammonium ions and the phenyl rings, respectively. Due to the different scattering cross sections of the ATPB and ATPB-D samples, the weight factors for ATPB differ from those in Eq. (11). They were obtained considering the incoherent scattering of the mobile hydrogen atoms in ammonium and phenyl groups.

The experimental data of ATPB and ATPB-D were reproduced using this model in an energy transfer window from -0.15 to 1.5 meV. The data were sorted into three groups, to obtain information about the Q dependence of the phenyl ring motions. The fit parameters were Δ_{02}^{Ph} and the jump distance of the phenyl ring motions, d^{Ph} , which defines A_{02}^{Ph} as given in Eq. (10). In Fig. 7 fit results are shown for ATPB-D (left-hand side) and ATPB (right-hand side) at $T = 300$ K, $\Delta E = 32$ μeV , and $Q = 1.3$ \AA^{-1} . For the fit parameters the values $d^{\text{Ph}} = 0.3$ \AA , which corresponds to a reorientation angle of about $8.4^\circ \pm 2^\circ$, and $\Delta_{02}^{\text{Ph}} = 0.06 \pm 0.02$ meV (jump rate of 0.03 ± 0.01 meV) were obtained. The fits shown here reproduce the experimental data well. The broader QE component due to ammonium ion reorientations around the C_3 axis is drastically reduced for the deuterated sample, having only about 20% of the intensity of the corresponding

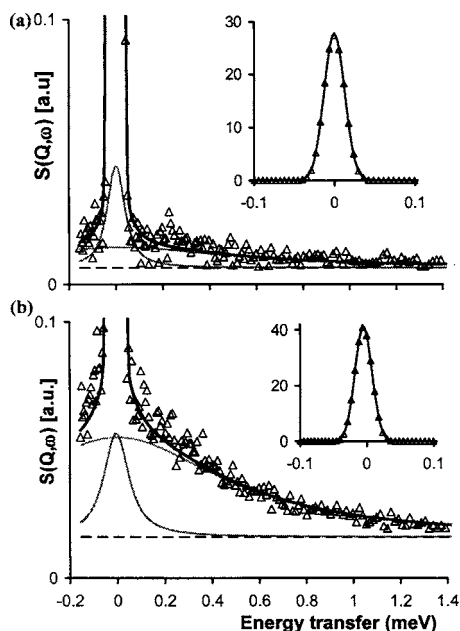


FIG. 7. The experimental QENS spectra at $T=300$ K with $\Delta E=32$ μeV and at an average Q value of 1.3 \AA^{-1} are shown (triangles) for ATPB-D (a) and ATPB (b). The fitted model (solid line) includes a contribution for the rotations of the ammonium ions around a C_3 axis (broader Lorentzian function) and another contribution for the reorientations of the phenyl rings (narrower Lorentzian function). The background was fitted as a straight line. The corresponding elastic components are shown in the insets.

component in ATPB. This is mainly due to the different cross sections of the NH_4 and $\text{N}(\text{D}_{0.77}\text{H}_{0.23})_4$, and also due to the different numbers of particles in the samples. It should be noted that the whole spectral intensity of the ATPB-D sample has about 70% of the intensity of the ATPB sample, because the samples have different scattering probabilities according to the different scattering cross sections and the different amounts of samples. The intensity of the narrower QE component is reduced for the ATPB-D sample by about 70% as well. This observation confirms that the narrower component indeed originates from reorientations of phenyl rings and is not due to ammonium-group motions. Due to the weak intensity and the poor statistical accuracy of this component, it was not possible to simultaneously determine the jump rate and the jump distance with good accuracy. Therefore within the framework of this study, it was not feasible to find the activation energy for this motion.

IV. CONCLUSIONS AND DISCUSSION

In this study the dynamics of the ammonium ions and of the phenyl rings, forming an aromatic H bond in ammonium tetraphenylborate, were studied in a comprehensive way with quasielastic incoherent neutron scattering. In a temperature range of 67 K $\leq T \leq 350$ K a reorientational motion of the ammonium ions around the C_3 axis was found. The correlation time for this motion varies from 1.5 ps ($\tau_3^{-1} = 0.44$ meV) at $T=350$ K to 150 ps ($\tau_3^{-1} = 0.0044$ meV) at $T=67$ K and the activation energy for these rotations was determined to be 3.14 kJ/mol. This result shows that the ammonium ions have to overcome an exceptionally low potential barrier to rotate.

It is interesting to note that the reorientational correlation time of the ammonium ion is also the mean residence time of the involved NH_4^+ protons in the corresponding hydrogen bonds. It therefore corresponds to the lifetime of the latter. Consequently, the related activation energy is simultaneous to that for the breaking H bonds. More precisely, it is that for the simultaneous rupture of three H bonds of the ammonium group occurring in connection with the C_3 -type reorientations. From this we deduce an average activation energy of 1.05 kJ/mol per single H bond, which indeed suggests a rather low potential barrier protecting that bond. Obviously, new H bonds are formed a short time later, whenever the reorienting ammonium group arrives in its next orientational equilibrium.

Another interesting result of this study concerns the details of the phenyl ring motions at temperatures above 200 K. We proved that an additional narrow QE component due to local diffusive reorientations of the phenyl rings is needed to explain the experimental data on the time scale of our QENS experiments. We have described these motions using again a reorientational jump-diffusion model. The reorientation angle and the jump rate of the reorientations of the phenyl rings increase with increasing temperatures. At room temperature these “librations” of the phenyl rings were found to have a reorientation angle of $\alpha = 8.4^\circ \pm 2^\circ$ and a correlation time of 22 ± 8 ps. This may be compared to the displacement parameters of the structural study of Steiner and Mason³ observed at room temperature: from these one would estimate a somewhat larger reorientation angle for the phenyl rings of approximately 13° , a qualitative agreement acceptable in view of the crude approximation made regarding the damped phenyl group librations. One may speculate that the very strong damping of the librational motion of the acceptors, making the transient H bond appear rather flexible, is caused by the continuously occurring alternation between rupture and formation of the H bonds connecting ammonium and phenyl groups.

Our results regarding the ammonium ion rotations around the C_3 axis are different from those of a previous study by Lucazeau *et al.*¹⁴ in two respects. These authors propose that the ammonium ion rotates around C_2 axes, with an activation energy of 2.9 kJ/mol. Our analysis regarding the activation energy is likely to be more precise, as we used a higher energy resolution in one part of the study, and a more appropriate model, which included also the contribution due to the diffusive reorientational motions of the phenyl rings to reproduce the experimental spectra at $T > 200$ K. The latter had not been seen by those authors, probably because the shape of their energy resolution function (largely based on a monochromator crystal reflection) was not sharp enough to distinguish the narrowest quasielastic component.

Previously, only presumptions about the geometry of the motions of the donor and acceptor of the aromatic H bond had been reported. Calculations and structural studies^{3,23–27} have indicated that the directionality of the aromatic H bond is extremely flexible. Our study provides now more precise information, showing that the donor rotates in a specific way, and the acceptor undergoes strongly damped librational mo-

tion with a partially diffusive character. Therefore this H bond can be considered as short lived and rather flexible.

ACKNOWLEDGMENTS

The authors are grateful to T. Steiner, who has proposed the subject of this study and provided the first powder sample of the hydrogenous compound used in the initial measurements. The authors also thank M. Russina and B. Urban for valuable assistance during the NEAT measurements, as well as N. Aliouane, C. Milne, and A. Chemseddine for the help with the sample characterization with x-ray diffraction and IR. One of the authors (N.J.) would also like to thank H. N. Bordallo for the fruitful discussions.

¹More precisely X-H...Ph.

²P. K. Bakshi, A. Linden, B. R. Vincent, S. R. Roe, D. Adhikesavalu, T. S. Cameron, and O. Knop, *Can. J. Chem.* **72**, 1273 (1994).

³T. Steiner and S. A. Mason, *Acta Crystallogr., Sect. B: Struct. Sci.* **56**, 254 (2000).

⁴QINS is a special case of the quasielastic neutron scattering (QENS) technique.

⁵W. Westerhaus, O. Knop, and M. Falk, *Can. J. Chem.* **58**, 1355 (1980).

⁶N. Jalarvo, Ph.D. thesis, Technische Universität Berlin, 2005, http://opus.kobv.de/tuberlin/volltexte/2005/1034/pdf/jalarvo_niina.pdf

⁷R. E. Lechner, *Physica B* **180–181**, 973 (1992).

⁸R. E. Lechner, *Physica B* **226**, 86 (1996).

⁹B. Ruffle, J. Ollivier, S. Longeville, and R. E. Lechner, *Nucl. Instrum. Methods Phys. Res. A* **449**, 322 (2000).

¹⁰B. Ruffle, *User Manual for FITMO2 (Tof-Data Analysing Program)* (BENSC, Berlin, 2000).

¹¹M. Bée, *Quasielastic Neutron Scattering* (Adam-Hilger, Bristol, 1988).

¹²T. Springer and R. E. Lechner, in *Diffusion in Condensed Matter*, 2nd ed., edited by P. Heitjans and J. Kärger (Springer, Berlin, 2005), Vol. 1, Chap. 3, pp. 93–164.

¹³J. Rubin, J. Bartolome, M. Anne, G. J. Kearley, and A. Mager, *J. Phys.: Condens. Matter* **6**, 8449 (1994).

¹⁴G. Lucazeau, A. Chahid, J. F. Bocquet, A. J. Dianoux, and M. P. Roberts, *Physica B* **164**, 313 (1990).

¹⁵R. Mukhopadhyay, P. S. Goyal, and C. J. Carlile, *Phys. Rev. B* **48**, 2880 (1993).

¹⁶R. S. Seymour and A. W. Pryor, *Acta Crystallogr., Sect. B: Struct. Crystallogr. Cryst. Chem.* **26**, 1487 (1970).

¹⁷R. E. Lechner, G. Badurek, A. J. Dianoux, H. Hervet, and F. Volino, *J. Chem. Phys.* **73**, 934 (1980).

¹⁸M. P. Roberts, G. Lucazeau, G. J. Kearley, and A. J. Dianoux, *J. Chem. Phys.* **93**, 8963 (1990).

¹⁹N. Jalarvo, R. E. Lechner, and A. Desmedt (unpublished).

²⁰M. Bee, A. J. Dianoux, and F. Volino, *Mol. Phys.* **51**, 221 (1984).

²¹S. Arrese-Igor, A. Arbe, A. Allegria, and J. Colmenero, *J. Chem. Phys.* **120**, 423 (2004).

²²C. M. Brown and J. L. Manson, *J. Am. Chem. Soc.* **124**, 12600 (2002).

²³G. A. Worth and R. C. Wade, *J. Phys. Chem.* **99**, 17473 (1995).

²⁴A. Aubry, *Acta Crystallogr., Sect. B: Struct. Crystallogr. Cryst. Chem.* **33**, 2573 (1977).

²⁵T. Steiner, S. A. Mason, and M. Tamm, *Acta Crystallogr., Sect. B: Struct. Sci.* **53**, 843 (1997).

²⁶K. Nakatsu, H. Yoshioka, K. Kunitomo, T. Kinugasa, and S. Uegi, *Acta Crystallogr., Sect. B: Struct. Crystallogr. Cryst. Chem.* **34**, 2357 (1978).

²⁷T. Steiner, E. B. Starikov, A. M. Amado, and J. J. Teixeira-Dias, *J. Chem. Soc., Perkin Trans. 2* **1996**, 67.